Performance of Field-Induced Directional Coupler Switches

V. R. Chinni, *Member, IEEE*, T. C. Huang, P. K. A. Wai, C. R. Menyuk, *Senior Member, IEEE*, and G. J. Simonis, *Member, IEEE*

Abstract—**Switching in a GaAs field-induced, three-waveguide straight directional coupler is studied theoretically. This device can be tuned externally by changing the voltage across the waveguides. Because of this tunability, the device has some very attractive features as a switching element. The performance change due to variations in the device parameters such as length, waveguide separation, waveguide width, and wavelength of operation is numerically computed. The effect of material absorption, input and output coupling, and asymmetric excitation are included in the performance evaluation. For a device length of 1400 μm, a crosstalk of −34 dB and a power transfer efficiency of −2 dB is predicted, while for the same device size a two-guide directional coupler is predicted a crosstalk of −13.4 dB. The device has a 400 nm voltage tunable bandwidth with a maximum crosstalk penalty of 3 dB.**

I. Introduction

DIRECTIONAL couplers are building blocks for many guided-wave devices in integrated optics. They have been used as switches, modulators, wavelength filters, polarization splitters, wavelength multiplexer-demultiplexers, and power dividers [1]–[5]. A directional coupler consists of a pair of closely spaced, parallel waveguides. The interaction of the evanescent fields of the guided modes in the individual waveguides causes power exchange between the coupled waveguides. The power transfer can be controlled by adjusting the synchronization and the coupling coefficient between the guides. An attractive feature of this coupling effect is its sensitivity to small changes in the values of the structure parameters (i.e., refractive indices, interguide spacing, guide width), allowing easy control of the energy exchange between the coupled waveguides by external factors such as electric, magnetic, and acoustic fields [6].

Recently, field-induced waveguides (FIG's) have been used to make a directional coupler switch [7]. We show the cross-section of a GaAs–AlGaAs field-induced waveguide in Fig. 1. The shaded region indicates the proton implantation that is used to confine the electric fields to the waveguide region and also to provide electric isolation between different waveguide regions. The lateral refractive index profile is also shown in Fig. 1. When no reverse bias is applied to the waveguide electrodes, the refractive index variation is negligible, and there is no optical confinement. When a reverse bias is applied to the waveguide electrodes, a high electric field appears at the p-n junctions underneath the electrodes. Due to both linear and quadratic electro-optic effects, the refractive index increases in the junction, so that the structure can now operate as an optical waveguide [8]. We show a field-induced straight directional coupler switch in Fig. 2. The waveguides are defined by the waveguide electrodes, and are separated by proton-implanted, electrically insulating regions. The light in the input, middle region can be coupled to either the left or right output regions by applying the appropriate reverse-biased voltage to the input and one of the output electrodes [7]. In contrast to conventional fixed waveguides, we can electrically turn on or off the optical confinement in these field-induced waveguides (FIG's). Furthermore, we can adjust the confinement factor, the propagation constant, and the net loss [8]. Since switching in FIG directional couplers is produced by turning on or off the waveguide region, rather than by slightly modifying the refractive index of the waveguide as in conventional directional couplers, it is possible to significantly reduce both the coupling length and the crosstalk. In FIG couplers the fabrication error can be compensated by tuning the voltage. FIG switches are cascadable and because of this small crosstalk, they are potentially useful in multilevel switching networks and routing systems [4]. We note that there has been no previous theoretical treatment of the straight three-guide FIG directional coupler that we are considering, and this configuration is important because bending losses are avoided and compact devices are possible.

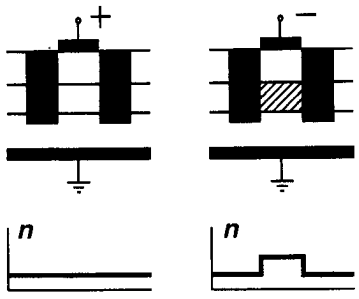

Fig. 1. Cross-section profile of a GaAs–AlGaAs field-induced waveguide.

Typically, directional couplers are narrow-band filters as the coupling length is a strong function of wavelength [2]. Narrow-

Manuscript received June 6, 1995. This work was supported by DOE. One of the authors, T. C. Huang, was supported by the NRC. Computational work was carried out at SDSC and NERSC.

V. R. Chinni and C. R. Menyuk are with the Department of Electrical Engineering, University of Maryland, Baltimore, MD 21228-5398 USA.

T. C. Huang and G. J. Simonis are with the Army Research Laboratory, Adelphi, MD 20783 USA.

P. K. A. Wai is with the Department of Electrical Engineering, University of Maryland, Baltimore, MD 21228-5398 USA. He is also with the Institute of Plasma Research, University of Maryland, College Park, MD 20742 USA.

IEEE Log Number 9414691.

band filters are useful for wavelength division multiplexing and demultiplexing, while wideband tunable switches are essential for signal routing in communication systems, where the signals might consist of several wavelengths. The tuning range for $LiNbO_3$-based optical waveguide directional couplers is several hundred angstroms [3]. In this paper, we show that FIG directional couplers can be tuned over a few thousand angstroms.

The rest of the paper is organized as follows: In Section II, we discuss the device geometry of the FIG directional coupler that we have chosen to study. In Section III, we discuss the device characteristics specific to this geometry. In Section IV, we evaluate the device's tolerance of variations in design parameters. In this section we also compute the tunable bandwidth range of these devices. In Section V, we discuss the performance of the proposed device and compare this performance with existing experimental results. Section VI presents a summary and conclusions.

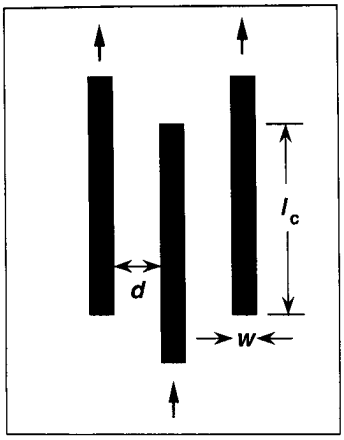

Fig. 2. Field-induced directional coupler. Light can be switched between two-output waveguides adjacent to the central waveguide by a change in the applied voltage. The parameter w is the waveguide width, l_c is the coupler length, and d is the gap between guiding regions.

II. Choice of Device Geometry

In this section, we discuss the geometry of the FIG directional coupler that we will examine and discuss this geometry's effect on the device performance. In a directional coupler switch, it is desirable to have waveguides whose confinement is relatively weak in order to reduce the coupling length between the guides, thereby reducing system size. Weakly guided field-induced waveguides are suitable candidates for use in directional couplers. In FIG's, the induced change in the refractive index is limited to approximately 0.005 for an applied reverse biased voltage range of 0–10 volts [8]. In the effective index range of 5×10^{-4} to 3×10^{-3}, the waveguides are only moderately confining and are single mode at the operating wavelength of 1.15 μm. This weak confinement implies that the waveguides are strongly coupled, so that the coupling lengths are small.

Conventional two-guide couplers have bends at the input and output. In order to minimize the overall size, small bend radii are preferred so that the waveguides can be brought into proximity and separated over short distances. However, small bends cause radiation loss. The radiation loss can be reduced by tightly confining the wave, but that in turn increases the coupling length and consequently the total device size [9]. Bends at the input also introduce a phase difference in the excited modes at the coupling region. In a fixed geometry, the coupling length can be adjusted to avoid degradation of the crosstalk due to the phase differences; but the phase differences are wavelength-dependent, so that at a fixed coupling length the crosstalk cannot be compensated at all wavelengths [10].

The proposed three-guide structure in Fig. 2 has straight input and output waveguides, and thus eliminates the need for bends. Although the FIG directional coupler switch consists of three waveguides, at any one time only the center and one of the output waveguides are switched on. The coupling lengths are therefore not $\sqrt{2}$ times longer than that of the two-guide coupler as is the case in other three-guide systems [9]. In a three-guide system, the crosstalk is defined as the ratio of the power in the desired output waveguide to the power in the unwanted output waveguide. This definition yields a lower crosstalk than the ratio between the power in the output waveguide to the power in the input waveguide because the spacing between the two output waveguides is larger than that between the output and input waveguides. In the absence of residual guiding the crosstalk is very low, and as we will show later, the crosstalk is typically 10–20 dB lower than that which can be obtained in a two-guide system. Our paper contains the first theoretical study of this structure.

III. Device Performance

In this section, we discuss the influence of geometric factors on the crosstalk, size, and loss of the device described in Section II when used as a switching element. We study the effect of waveguide width, waveguide separation, material absorption, and the index of refraction on the crosstalk, coupling length, and loss of the three-guide FIG directional coupler switch. We shall compare the performance of the three-guide FIG coupler to that of a traditional two-guide symmetric directional coupler.

Directional couplers can be analyzed using either the normal mode or coupled mode approaches [11]. Coupled mode theory gives an accurate description of power transfer in weakly coupled devices, but its accuracy is limited in strongly coupled devices as the theory does not properly account for the deformation of the modes of the individual waveguides. Normal mode analysis is applicable for strong coupling; however, it is cumbersome to include radiation effects in normal mode analysis, and it is difficult to analyze systems with multiple waveguides. Numerical simulations, particularly beam propagation methods, have been used extensively to analyze and design directional couplers [12], [13]. This approach is applicable when guiding is weak, can include the effects of loss and radiation, and is applicable to asymmetric multiwaveguide systems. For the analysis of the proposed waveguide structure, we chose a finite difference beam propagation method (FDBPM) based on the Crank–Nicholson algorithm [14]. We use the effective index method to reduce the three-dimensional structure to a two-dimensional structure [15], and

we implement transparent boundary conditions at the edges of the computational window [16].

A. Absorption

In lossless waveguides, the coupling length that yields the maximum power transfer also yields the minimum crosstalk. Guided modes suffer loss in FIG's, and the absorption in the guiding region is different from that in the surrounding region [7], [8]. Absorption in these waveguides is mainly due to inhomogeneities and proton implantation. As a result, even and odd modes experience different amounts of absorption, and, consequently, power cannot be completely switched to the output waveguides, causing crosstalk. Therefore, the coupling length that yields the minimum crosstalk is different from that which yields the maximum power transfer [17].

As an example, we evaluate the power transfer characteristics of a two-guide symmetric FIG directional coupler with and without loss. Fig. 3 shows the transfer of power between the two waveguides as a function of propagation distance. We show power in the input and output waveguides and the total power as functions of device length. The dashed curves correspond to the lossless case and the solid curves correspond to the lossy case. The waveguide width is 4 μm, the waveguide separation is 2 μm, and the wavelength is 1.15 μm. The index of the cladding is 3.400 and the index of the waveguide is 3.402. When we include absorption, the absorption coefficients are 1 cm^{-1} in the waveguide and 5 cm^{-1} in the surrounding region [7], [8]. Throughout this paper we will use this set of waveguide parameters for both the three-guide and two-guide directional couplers unless stated otherwise.

In Fig. 3, we find that the length at which we achieve maximum power in the output waveguide of a coupler with absorption (point A) differs from the length at which we achieve minimum power in the input waveguide (point B). Near points A and B, the rate of power absorption is larger than the power transfer between the waveguides. Even though there is power being coupled from the input waveguide to the output waveguide, there is no increase in power at the output waveguide as the loss is larger than the gain at that point. The difference between the lengths at which maximum power transfer occurs and the lowest crosstalk is achieved can be larger than 100 μm. When absorption is not included, the coupling length is 1452 μm and the crosstalk is -10.7 dB. When absorption is included, the maximum power transfer point shifts to 1250 μm and the minimum crosstalk is at a coupling length of 1455 μm with a value of -10.2 dB.

As demonstrated in the above example, the absorption alters the crosstalk and the coupling length significantly [17]. Therefore, we will include material absorption in our analysis. In the rest of this paper, coupling length refers to the length for the minimum crosstalk.

B. Coupling Length

The coupling length of a device determines its size and consequently the switching speed. In a directional coupler, the coupling length is a function of the geometric parameters and the wavelength of operation. We calculate the coupling

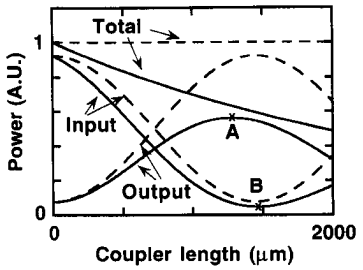

Fig. 3. Transfer characteristics of a symmetric two-guide directional coupler (A) (dashed line) with no absorption and (B) (solid line) with absorption as a function of propagation length. Power in the input and output waveguides and the total power are shown as a function of device length. Because of absorption, the length corresponding to maximum power transfer is different from the length for lowest crosstalk.

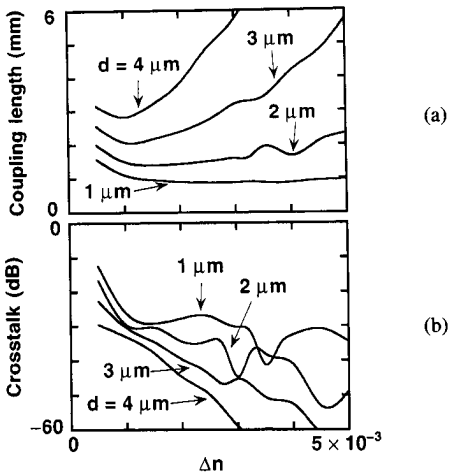

Fig. 4. (a) The coupling length and (b) minimum crosstalk of a three-guide, FIG directional coupler as a function of index difference in the waveguide region (Δn) for different waveguide separations d.

lengths in the three-guide FIG directional coupler switch with different waveguide indexes and interguide spacings, and we show the results in Fig. 4(a). For comparison, we show the coupling lengths in a two-guide symmetric directional coupler in Fig. 5(a).

As shown in Figs. 4(a) and 5(a), we find that when the waveguide index difference Δn increases, the coupling length first decreases, reaching a minimum and then increases. The maximum difference between the even and odd mode effective indexes is limited by the index difference. The effective indices of the guided modes are smaller than the waveguide index and larger than the cladding index. The coupling length l_c is given by

$$l_c = \frac{\pi}{\beta_e - \beta_o} = \frac{\lambda}{2(n_e - n_o)}, \tag{1}$$

where $n_c < n_o < n_e < n_g$, and β_e and β_o are the propagation constants of the even and odd modes of the directional coupler structure, λ is the operating wavelength, and n_e and n_o are effective indices of the even and odd modes. The parameters n_c and $n_g = n_c + \Delta n$ are indices of the cladding and the waveguide. Since $n_e - n_o < \Delta n$, it follows

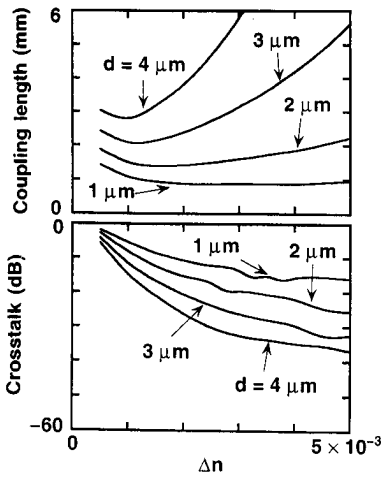

Fig. 5. (a) The coupling length and (b) minimum crosstalk of a two-guide symmetric, directional coupler as a function of index difference in the waveguide region (Δn) for different waveguide separations d.

that $l_c > \lambda/\Delta n$. As Δn goes to zero, n_o approximates n_c while n_e approximates n_g, so that l_c is proportional to $1/\Delta n$. Consequently, in the limit when Δn is small, the coupling length increases as the waveguide index decreases. As Δn becomes larger, the coupling length begins to increase due to tighter mode confinement and smaller field overlap. From Figs. 4(a) and 5(a), we find that the coupling lengths of the three-guide FIG directional coupler and a two-guide symmetric coupler are similar. The oscillations on the curves in Fig. 4(a) are mainly due to radiation and are explained in the next subsection.

C. Crosstalk

In directional couplers, the crosstalk has been attributed to the asymmetry of the waveguides [18], absorption loss [17], nonoptimal coupling length [19], unequal excitation of the symmetric and asymmetric modes at the input [20], coupling of radiation modes to the output, and fabrication variations. Even under ideal conditions with an optimal coupling length, symmetric structure, and no absorption loss, asymmetry in the excitation of even and odd modes results in crosstalk. The asymmetry exists because the propagation constants of the even and odd modes are different and correspondingly the power coupled from the input waveguide to each of these modes is different. This crosstalk depends on the refractive index and spacing between the waveguides. It determines the minimum achievable crosstalk [20].

Figs. 4(b) and 5(b) show the minimum achievable crosstalk in the three-guide FIG directional coupler and the two-guide symmetric directional coupler respectively. The parameters used are the same as those in Figs. 4(a) and 5(a). For moderate values of Δn and large waveguide separations, the crosstalk decreases when Δn increases because of the decreased asymmetric excitation of even and odd modes. When Δn and the waveguide separation are small, the two active waveguides together behave almost like a single wider waveguide; the difference between the odd and even mode becomes significant, and the coupling of input power into the odd mode decreases. A large fraction of the input power is therefore lost to radiation at the input transition region. When the odd mode ceases to exist, the power coupled into that mode is zero. This difference in the amount of power that is coupled into the two modes when Δn is small gives rise to a significant amount of crosstalk.

From Figs. 4(b) and 5(b), we conclude that the crosstalk in the three-waveguide FIG directional coupler switch is much smaller than that in a two-guide directional coupler. The oscillations of the crosstalk in a three-guide FIG device is due to the radiation present in the nonguiding, unintended output waveguide and the appearance of higher-order modes when $\Delta n \geq 0.003$. The appearance of higher-order modes lowers the crosstalk significantly in a three-guide directional coupler because more of the input power is coupled into the guided modes. As a result the power coupled to radiation decreases, reducing the crosstalk. The appearance of higher-order modes does not have as much impact in a two-guide directional coupler because here the crosstalk is defined as the ratio of power in the guided regions where the impact of radiation will be smaller.

D. Power Transfer Efficiency

The power loss in the device can be due to the radiation, material absorption, and power coupled to the unwanted waveguides. In the case presented here, material absorption dominates, and consequently the device loss is a strong function of the coupling length. Accordingly, we observed that the power transfer efficiency defined as the ratio of power in the output waveguide to the input power, is inversely proportional to the coupling length of the device. When the material absorption is small, the power transfer efficiency is high as the other losses are also small.

IV. Tolerance of Fabrication Variations

In this section, we analyze the performance tolerances of a FIG directional coupler switch as a function of fabrication variations in its geometrical parameters, i.e., waveguide length, separation, and width. We also discuss the tunable wavelength wideband characteristics of this device.

Crosstalk is a strong function of the device length. When the device length equals its coupling length, we obtain the minimum possible crosstalk. When the device length deviates from the coupling length, the crosstalk increases. Fig. 6 shows the crosstalk of the three-guide directional coupler as a function of the device length. The crosstalk variation due to nonoptimal coupling can be compensated by using the external voltage to tune the refractive index of the waveguides. The minimum crosstalk obtainable is shown as the solid curve in Fig. 6. We observe that deviation of the device length from the design length will result in variation of the crosstalk as tuning of Δn cannot completely compensate for the deviations. In this device, it is possible to decrease the device length from the initially designed value of 1400 μm to 1300 μm if an increased crosstalk of less than 2 dB is tolerable. Increase in the device length up to 1800 μm only results in reduced crosstalk.

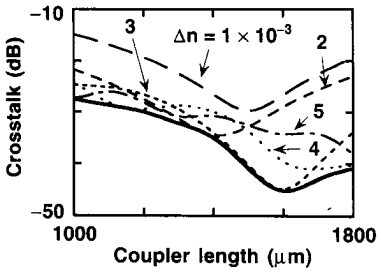

Fig. 6. Effect of coupling length on the crosstalk performance in the three-guide FIG directional coupler switch with waveguide refractive index differences (Δn) of 0.001, 0.002, 0.003, 0.004, and 0.005. The minimum tunable crosstalk is shown with a solid curve.

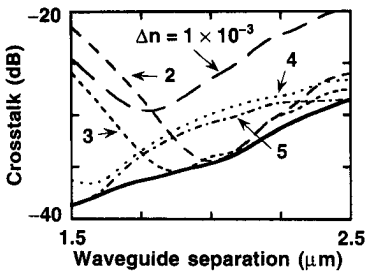

Fig. 7. Effect of waveguide separation on the crosstalk performance in the three-guide FIG directional coupler switch with waveguide refractive index differences (Δn) of 0.001, 0.002, 0.003, 0.004, and 0.005. The minimum tunable crosstalk is shown with a solid curve.

Due to fabrication errors, the distance between the waveguides in the coupler can be slightly different from the designed value. The effect of variable spacing has been analyzed in [5]. The crosstalk variation due to deviation in the interguide spacing can be compensated by altering the voltage across the waveguides. Because the tuning cannot completely compensate for the crosstalk, the crosstalk of the modified structure, even when minimized, is different from the crosstalk expected from the designed structure. Fig. 7 shows the effect of variation in the waveguide separation as a function of the waveguide refractive index difference. The crosstalk is measured at a coupler length of 1400 μm. We show the minimum obtainable crosstalk as a solid curve in Fig. 7. An increase of the waveguide separation from 2 μm by 10 percent results in a crosstalk increase of 2 dB, while a decrease in the waveguide separation results in decreased crosstalk.

In general, the width of the waveguides can be different from the designed value or may even vary along the length of the guiding region. The change in the waveguide width alters the mode profiles, which in turn affects the coupling length and changes the crosstalk. We analyzed the effects of variation in the waveguide width on the performance of a directional coupler and computed the effective crosstalk variation after waveguide index tuning has been performed, and the results are shown in Fig. 8. We show the minimum achievable crosstalk as a solid curve.

We find from Fig. 8 that the effect of small fabrication changes on the waveguide width on the order of 5% can be compensated by proper tuning of the voltage and the resulting crosstalk increase is less than 2 dB. If the waveguide width increases by 10% from 4 μm, the crosstalk increase is about 4 dB, while a decrease in the waveguide width only lead to a decrease in crosstalk.

In FIG's, the built-in voltage across the metallic junctions causes a small change in refractive index along the waveguide even in the absence of an external field, leading to a weak residual guiding. Residual guiding in the unwanted output waveguide of a three-guide coupler leads to an increase in crosstalk. Forward biasing the waveguide can reduce the built-in voltage, but it may not eliminate the residual guiding. For a small residual guide index, the length required to transfer power from the input waveguide to the residual waveguide is much longer than the coupling length required for power transfer into the intended output port. Therefore, the power

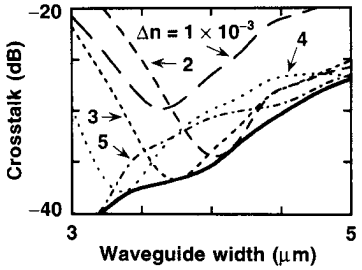

Fig. 8. Effect of waveguide width on the crosstalk in the three-guide FIG directional coupler switch with waveguide refractive index differences (Δn) of 0.001, 0.002, 0.003, 0.004, and 0.005. The minimum tunable crosstalk is shown with a solid curve.

coupled into the unwanted port is usually small and so is the crosstalk degradation due to residual guiding.

Both the refractive index of the material and the mode confinement in a waveguide depends on the wavelength. In FIG directional couplers, the change in crosstalk due to wavelength variation, as with other variations, can be minimized by tuning the device voltage. The coupling length in a two-guide symmetric directional coupler operating at a wavelength λ is given by (1) and all the parameters in this equation are functions of λ. When the wavelength increases, the coupling length l_c decreases due to stronger coupling between the modes. In our calculations, we assumed that the change in refractive index of the material with wavelength is small. This assumption is valid except near the band gap of the material, and at 1.15 μm, the wavelength that we consider in all our examples, we are far from the bandgap of GaAs.

Our results show that the coupling length and crosstalk depend sensitively on the wavelength. Fig. 9 shows the crosstalk of a device with a length of 1400 μm as a function of wavelength. By changing the external voltage we can compensate the effects due to wavelength variations. The solid curve shows the minimum achievable crosstalk as a function of wavelength. Because the variation in crosstalk is small, the switch can operate over a considerable wavelength range without a significant increase in the crosstalk. If a 3 dB increase in crosstalk is tolerable, the wavelength range is 400 nm. This range is an order of magnitude higher than that has been reported for $LiNbO_3$ directional couplers [3]. For a tolerance of 5 dB variation in the crosstalk, the range is over

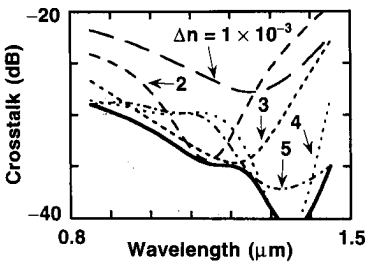

Fig. 9. Crosstalk performance as a function of operating wavelength for a device of length 1400 μm in the three-guide FIG directional coupler switch with waveguide refractive index differences (Δn) of 0.001, 0.002, 0.003, 0.004, and 0.005. The minimum tunable crosstalk is shown with a solid curve.

500 nm which covers a large part of the optical spectrum used in integrated optics applications.

V. Comparison with Experiments

We now compare our results to the experimental device studied in [7]. This device operated at 1.15-μm wavelength with a 4 μm waveguide width and a 2-μm waveguide separation at an applied bias of 8 volts ($\Delta n \approx 0.002$), which were the base values that we used in our analysis in the preceding sections.

For this specific set of parameters, we find that the coupling length is 1440 μm and the minimum achievable crosstalk is -34 dB. There is a 2-dB variation in crosstalk for a variation of 100-μm variation in the device length, or for a 10% variation in waveguide separation, or for a 5% variation in waveguide width variation. The wavelength of operation can be tuned from 1000–1400 nm with a 3-dB tolerance in the crosstalk. The tunable wavelength range is from 900–1400 nm with a 5-dB tolerance in the crosstalk.

The coupling length of the above device is experimentally found to be 1400 μm, which is in the good agreement with the theoretical results. The experimentally measured minimum crosstalk is -12 dB in contrast to the theoretical prediction of -34 dB. The discrepancy between the measured and numerical results may be due to radiation and nonideal input coupling. The radiation excited at the interface of the input waveguide with the coupling region is not orthogonal to the eigenmodes of the output waveguides; therefore, radiation can couple into the output waveguides. The scattering in the directional coupler due to inhomogeneities would also increase the crosstalk. The crosstalk performance degradation can also be due to significantly higher absorption losses in the cladding region due to proton implantation. Nonuniform absorption across the device structure can deteriorate the performance significantly [17].

In this paper, we did not consider the possibility of tuning the indices of the waveguides individually, as in a complex switching array, it is desirable to reduce the number of output pins. Also for cascadability of the device and for good mode matching between different elements, the waveguides should have same cross section and refractive index profiles.

VI. Summary and Conclusion

In this paper, we use the beam propagation method to design a three-guide FIG directional coupler and then study the effects of fabrication errors. We determined the voltage tuning that is necessary to counter the crosstalk deterioration due to the variations in different waveguide fabrication parameters. We compared the performance of the three-guide FIG directional coupler to a two-guide directional coupler switch. The FIG directional coupler has short coupling lengths and low crosstalk. The tuning range for a given acceptable performance degradation is determined. The tunable bandwidth of a FIG directional coupler is calculated to be 400 nm for a variation of 3 dB in crosstalk, whereas the tuning range for a $LiNbO_3$-based optical waveguide directional couplers is only a several hundred angstroms [3]. For a device length of 1400 μm, a crosstalk of -34 dB and a power transfer efficiency of -2 dB is predicted, while for the same device size a two-guide directional coupler has a predicted crosstalk of -13.4 dB. We believe that this type of structure with its unique capability to compensate the effects of fabrication errors or wavelength variations has the potential to be a compact, cascadable, fast, low-crosstalk, and robust integrated optical switch element.

References

[1] R. C. Alferness, "Guided-wave devices for optical communication," *IEEE J. Quantum Electron.*, vol. QE-17, pp. 946–959, 1981.
[2] A. Villeneuve, K. Al-Hemyari, J. U. Kang, C. N. Ironside, J. S. Aitchison, and G. I. Stegeman, "Demonstration of all-optical demultiplexing at 1555 nm with an AlGaAs directional coupler," *Electron. Lett.*, vol. 29, pp. 721–722, 1993.
[3] R. C. Alferness and R. V. Schmidt, "Tunable optical waveguide directional coupler filter," *Appl. Phys. Lett.*, vol. 33, pp. 161–163, 1978.
[4] A. Jajszczyk, "Directional coupler-based planar concentrator networks," *Electron. Lett.*, vol. 26, pp. 886–887, 1990.
[5] T. Findakly and C-L. Chen, "Optical directional couplers with variable spacing," *Appl. Opt.*, vol. 17, pp. 769–773, 1978.
[6] T. Tamir, *Integrated Optics.* New York: Springer-Verlag, 1979.
[7] T. C. Huang, G. J. Simonis, and L. A. Coldren, "Directional coupler optical switch constructed from field-induced waveguides," *Electron. Lett.*, vol. 28, pp. 2288–2289, 1992.
[8] T. C. Huang, Y. Chung, L. A. Coldren, and N. Dagli, "Field-induced waveguides and their application to modulators," *IEEE J. Quantum Electron.*, vol. 29, pp. 1131–1143, 1993.
[9] H. A. Haus and C. G. Fonstad, Jr., "Three-waveguide couplers for improved sampling and filtering," *IEEE J. Quantum Electron.*, vol. QE-29, pp. 2321–2325, 1981.
[10] J. Weber, L. Thylen, and S. Wang, "Crosstalk and switching characteristics in directional couplers," *IEEE J. Quantum Electron.*, vol. 24, pp. 537–548, 1988.
[11] E. Marom, O. G. Ramer, and S. Ruschin, "Relation between normal-mode and coupled-mode analyses of parallel waveguides," *IEEE J. Quantum Electron.*, vol. QE-20, pp. 1311–1319, 1984.
[12] M. D. Feit and J. A. Fleck, Jr., "Propagating beam theory of optical fiber cross coupling," *J. Opt. Soc. Am.*, vol. 71, pp. 1361–1372, 1981.
[13] P. Sansonetti, E. C. Caquot, and A. Carenco, "Design of semiconductor electro-optic directional coupler with the beam propagation method," *J. Lightwave Technol.*, vol. 7, pp. 385–389, 1989.
[14] Y. Chung and N. Dagli, "An assessment of finite difference beam propagation method," *IEEE J. Quantum Electron.*, vol. 26, 1335–1339, 1990.
[15] G. B. Hocker and W. K. Burns, "Mode dispersion in diffused channel waveguides by the effective index method," *Appl. Opt.*, vol. 16, pp. 113–118, 1977.
[16] G. R. Hadley, "Transparent boundary condition for the beam propagation method," *IEEE J. Quantum Electron.*, vol. 28, pp. 363–370, 1992.
[17] V. R. Chinni, T. C. Huang, P. K. A. Wai, C. R. Menyuk, and G. J. Simonis, "Crosstalk in a lossy directional coupler switch," *J. Lightwave Technol.*, vol. 13, pp. 1530–1535, July 1995.
[18] R. C. Alferness, "Guided-wave devices for optical communication," *IEEE J. Quantum Electron.*, vol. QE-17, pp. 946–959, 1981.
[19] D. Marcuse, *Light Transmission Optics.* Princeton, NJ: Van Nostrand Reinhold, 1972.
[20] K. L. Chen and S. Wang, "Crosstalk problems in optical directional couplers," *Appl. Phys. Lett.*, vol. 44, pp. 166–168, 1984.

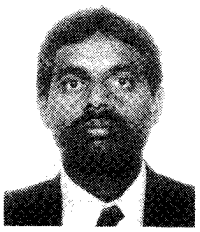

V. R. Chinni (S'89–M'95) received the Ph.D. degree in 1994 from the University of Maryland, Baltimore, in the areas of computational photonics and integrated optics. His doctoral work included simulation, modeling, and design of integrated optical waveguide devices.

Prior to his doctoral work, he was involved in design and development of high-speed, long-distance, fiber-optic communication systems at Indian Telephone Industries, Bangalore. Since 1995, he has been working with AT&T Bell Laboratories, Middletown, NJ.

T. C. Huang received the B.S. degree in physics from Jilin University, Jilin, China, in 1982, and the M.S. and Ph.D. degrees in electrical engineering from the University of California, Santa Barbara, in 1987 and 1991, respectively.

During his Ph.D. research, he worked on the design, fabrication, modeling, and characterization of integrated optoelectronic devices in III–V compound semiconductors. From 1991–1994, he was at the Army Research Laboratory, Adelphi, MD, where his work was concerned with optoelectronic components and their applications to lightwave communications and optical signal processing systems. Currently, he is at the Hewlett-Packard Laboratories, Palo Alto, CA, engaged in work on optoelectronic devices and systems for parallel optical data link.

P. K. A. Wai was born in Hong Kong on January 22, 1960. He received the B.S. degree from the University of Hong Kong, in 1981, and the M.S. and Ph.D. degree from the University of Maryland, College Park, in 1985 and 1988, respectively.

In 1988, he joined Science Applications International Corporation (SAIC) as a research scientist, where he worked on the Tethered Satellite project. Since 1990, he has been a research associate with the Laboratory of Computational Photonics in the Electrical Engineering Department at the University of Maryland, Baltimore County. His research interests include theory of solitons, modeling of fiber lasers, simulation of integrated optical devices, long distance fiber optic communication, and neural networks.

C. R. Menyuk (SM'88) was born on March 26, 1954. He received the B.S. and M.S. degrees from MIT, in 1976, and the Ph.D. degree from UCLA, in 1981.

He has worked as a research associate at the University of Maryland, College Park, and at Science Applications International Corporation in McLean, VA. In 1986, he became an associate professor in the Department of Electrical Engineering at the University of Maryland, Baltimore County (he was the founding member of this department). In 1993, he was promoted to Professor. For the last few years, his primary research areas has been theoretical and computational studies of nonlinear and guided-wave optics. Computer codes that he wrote to model the nonlinear propagation of light in optical fibers have been used by industrial, government, and university research groups throughout the United States.

Dr. Menyuk is a member of APS, OSA, and SIAM.

G. J. Simonis (M'78) was born in Wisconsin Rapids, WI, on November 9, 1946. He received the B.S. degree in physics/mathematics from Wisconsin State University, Platteville, in 1968, and the Ph.D. degree in physics (solid-state Raman spectroscopy) from Kansas State University, in 1973.

He served as a research physicist in the U.S. Army at Harry Diamond Laboratories (which became a part of the Army Research Laboratory), in 1994. His research activities have included long wavelength infrared nonlinear processes in liquids, hydrogen fluoride gas lasers, far-infrared optically pumped gas lasers, far-infrared/millimeter wave properties of materials, and III–V semiconductor optoelectronics. Recent activities include optoelectronic control of microwaves and hybride and monolithic optoelectronic integrated circuits.

Dr. Simonis is a member of OSA, APS, and SPIE.